Geomagnetic Orbit Determination Using Fuzzy Regulating Unscented Kalman Filter

CHEN Guifang[1,2], *YU Feng*[1,2*], *ZONG Hua*[3], *WANG Run*[1,2]

1. College of Astronautics, Nanjing University of Aeronautics and Astronautics, Nanjing 211106, P.R. China;
2. Key Laboratory of Space Photoelectric Detection and Perception (Nanjing University of Aeronautics and Astronautics), Ministry of Industry and Information Technology, Nanjing 210016, P.R. China;
3. National Key Laboratory of Science and Technology on Aerospace Intelligent Control, Beijing 100854, P.R. China

(Received 30 June 2020; revised 9 November 2020; accepted 15 November 2020)

Abstract: Geomagnetic orbit determination fits for nanosatellites which pursue low cost and high-density ratio, but one of its disadvantages is the poor position accuracy introduced by magnetic bias. Here, a new method, named the fuzzy regulating unscented Kalman filter (FRUKF), is proposed. The magnetic bias is regarded as a random walk model, and a fuzzy regulator is designed to estimate the magnetic bias more accurately. The input of the regulator is the derivative of magnetic bias estimated from unscented Kalman filter (UKF). According to the fuzzy rule, the process noise covariance is adaptively determined. The FRUKF is evaluated using the real-flight data of the SWARM-A. The experimental results show that the root-mean-square (RMS) position error is 3.1 km and the convergence time is shorter than the traditional way.

Key words: geomagnetic orbit determination; unscented Kalman filter (UKF); fuzzy regulator; magnetic bias; international geomagnetic reference field (IGRF)

CLC number: V44 **Document code:** A **Article ID:** 1005-1120(2021)04-0695-09

0 Introduction

The magnitude and vector of the geomagnetic field are relevant to the position and attitude of satellite related to the Earth. Thus, the geomagnetic field can be utilized for orbit determination[1].

The geomagnetic orbit determination was first tested by Pisiaki in 1993[2]. The measurement was the magnitude of the geomagnetic field, and an extended Kalman filter (EKF) was designed. The real-flight data from the magnetic field satellite (MAGSAT) was used in his experiment, and the results showed that the position error was about 8 km. The geomagnetic field model selected the international geomagnetic reference field (IGRF), which is difficult in calculation and linearization. Thus, a polynomial geomagnetic model was proposed[3], and the experiment showed its validity by using real-flight data. As the geomagnetic orbit determination system is non-linear, the unscented Kalman filter (UKF) can improve the orbit determination accuracy. Besides, a sigma-point batch filter (UBF) was proposed and the positioning accuracy was 1—2 km. This method was validated by using the data from the satellite Challenging Minisatellite Payload (CHAMP)[4]. However, the data the batch filter used should be collected for days, which is not proper for real-time orbit determination. To improve the observability of the orbit determination system, researchers also took other observations into account. The sensors they employed included horizon sensor[5], sun sensor[3,6-7], redshift[6] and star sensor[8].

The accuracy of IGRF limits the performance of the geomagnetic orbit determination system[7]. Pi-

*Corresponding author, E-mail address: yufeng@nuaa.edu.cn.

How to cite this article: CHEN Guifang, YU Feng, ZONG Hua, et al. Geomagnetic orbit determination using fuzzy regulating unscented Kalman filter[J]. Transactions of Nanjing University of Aeronautics and Astronautics, 2021, 38(4): 695-703.
http://dx.doi.org/10.16356/j.1005-1120.2021.04.015

siaki defined an external time-varying magnetic field and perturbations from the 1985 IGRF model of the internal field with 130 coefficients, and the coefficients are considered as state variables[9]. However, this method is too complex for the restricted calculation capacity in orbit. Define the magnetic bias as the difference between the calculated geomagnetic data produced by solving the geomagnetic field model and the geomagnetic data produced by magnetometer. Therefore, the magnetic bias includes the magnetometer error, geomagnetic model error and remanence. In the attitude determination algorithm, the magnetic bias can be reduced by two-step[10] or three-step algorithm[11]. In the geomagnetic orbit determination, the magnetic bias is usually modeled as a random walk and estimated as a state variable. Researchers investigated the relationship between the geomagnetic model error and the geographic latitude, and then removed the geomagnetic model error in orbit determination processing[12]. However, this method cannot be used to eliminate the influence introduced by magnetometer error and remanence.

This paper proposes a fuzzy regulating UKF (FRUKF) to realize the geomagnetic orbit determination. The observation of the system is the geomagnetic field magnitude, which is estimated by IGRF. The magnetic bias is modeled as a random walk, and then a fuzzy regulator is designed to improve its estimating accuracy. The input of this regulator is the difference between two neighboring magnetic biases estimated by the UKF. After the fuzzy processing, a process noise covariance is determined on line. Experiments are performed with the real-flight data from SWARM-A, and the results show that the accuracy of geomagnetic orbit determination using FRUKF is better than the traditional method and the convergence time is also shorter.

1 Geomagnetic Orbit Determination Model

1.1 Orbit dynamics model

Since the input of IGRF is described in the Earth-fixed coordinates, the orbit dynamics model considered the J2 effect can be described as

$$\begin{cases} \dot{x}=v_x \\ \dot{y}=v_y \\ \dot{z}=v_z \\ \dot{v}_x= \\ \quad \left(-\dfrac{\mu}{r^3}\left[1-J_2\left(\dfrac{R_e}{r}\right)^2\left(7.5\dfrac{z^2}{r^2}-1.5\right)\right]+\omega^2\right)x+ \\ \quad 2\omega\cdot v_y \\ \dot{v}_y= \\ \quad \left(-\dfrac{\mu}{r^3}\left[1-J_2\left(\dfrac{R_e}{r}\right)^2\left(7.5\dfrac{z^2}{r^2}-1.5\right)\right]+\omega^2\right)y- \\ \quad 2\omega\cdot v_x \\ \dot{v}_z=-\dfrac{\mu}{r^3}\left[1-J_2\left(\dfrac{R_e}{r}\right)^2\left(7.5\dfrac{z^2}{r^2}-4.5\right)\right]z \end{cases} \tag{1}$$

where $\boldsymbol{r}=[x,y,z]^{\mathrm{T}}$ and $\boldsymbol{v}=[v_x,v_y,v_z]^{\mathrm{T}}$ are the position and velocity of satellite respectively. μ is the Earth gravitational constant; r the magnitude of the vector $\boldsymbol{r}$; R_e the equatorial radius of Earth; and ω the Earth rotation angular velocity.

1.2 Measurement model

Choose the IGRF as the geomagnetic model, and the geomagnetic potential V can be expressed as

$$V=a\sum_{n=1}^{N}\sum_{m=0}^{n}\left(\frac{R_e}{r}\right)^{n+1}FP_n^m(\cos\theta) \tag{2}$$

where $a=6\,371.2$ km, $N=13$, $F=g_n^m\cos(m\lambda)+h_n^m\sin(m\lambda)$. g_n^m and h_n^m are the Gauss coefficients. λ is the longitude and θ the geocentric co-latitude. $P_n^m(\cos\theta)$ are the Schmidt quasi-normalized associated Legendre functions of degree n and order m[13].

Thus, the northward, eastward, and inward components of the geomagnetic field are

$$\begin{cases} B_x=\displaystyle\sum_{n=1}^{N}\sum_{m=0}^{n}\left(\frac{R_e}{r}\right)^{n+2}F\frac{\mathrm{d}P_n^m(\cos\theta)}{\mathrm{d}\theta} \\ B_y=\displaystyle\sum_{n=1}^{N}\sum_{m=0}^{n}\frac{m}{\sin\theta}\left(\frac{R_e}{r}\right)^{n+2}FP_n^m(\cos\theta) \\ B_z=-\displaystyle\sum_{n=1}^{N}\sum_{m=0}^{n}(n+1)\left(\frac{R_e}{r}\right)^{n+2}F\frac{\mathrm{d}P_n^m(\cos\theta)}{\mathrm{d}\theta} \end{cases} \tag{3}$$

The satellite's attitude is needed if the observation is geomagnetic field vector[8]. However, the accuracy of the attitude determination of some nanosatellites is too poor to meet the requirement of geomagnetic orbit determination. Therefore, the magnitude of geomagnetic field is used. The measurement model can be described as

$$B_m = \sqrt{B_x^2 + B_y^2 + B_z^2} + B_b + \eta \tag{4}$$

where B_m is the geomagnetic measurement obtained from the magnetometer, η the zero-mean Gaussian noise, and B_b the magnetic bias. B_b can be modeled as a random walk as

$$\dot{B}_b = a_b \tag{5}$$

where a_b is the zero-mean Gaussian noise.

Then, B_b is considered as a state variate in the UKF. Thus, the state vector can be rewritten as

$$\boldsymbol{x} = [\boldsymbol{r}^T, \boldsymbol{v}^T, B_b]$$

2 FRUKF Design

2.1 UKF design

EKF is an efficient tool for orbit determination. However, the neglection of higher order terms in Taylor expansion calculation is an approximation process. The UKF improves the estimating accuracy by using so-called sigma points. The sigma points are a minimal set of points that is capable to capture the true mean and covariance of the state vector. This approach is called unscented transform (UT).

According to the Eqs.(1, 4), the nonlinear discrete-time system of the geomagnetic orbit determination can be summarized as

$$\begin{cases} \boldsymbol{x}_{k+1} = \boldsymbol{f}(\boldsymbol{x}_k, \boldsymbol{w}_k, t_k) \\ z_k = h(\boldsymbol{x}_k, \eta_k, t_k) \end{cases} \tag{6}$$

where $\boldsymbol{x}_k$ is the state vector at t_k, $\boldsymbol{w}_k = [f_{x,k}, f_{y,k}, f_{z,k}, a_{b,k}]$ is the process noise at t_k, η_k is the measurement noise at t_k. $\boldsymbol{w}$ and $\boldsymbol{\eta}$ are the zero-mean Gaussian noise vectors. Then, the covariance matrix of $\boldsymbol{w}$ is denoted as $\boldsymbol{Q}$, and the covariance matrix of $\boldsymbol{\eta}$ is denoted as $\boldsymbol{R}$.

The equations of UKF are summarized in Table 1[14], where $\lambda = \alpha^2(n+k) - n$ is the composite scaling parameter, n the dimension of $\boldsymbol{x}^a$, and $W_i^{(m)}$ and $W_i^{(c)}$ are calculated by

$$\begin{cases} W_0^{(m)} = \lambda/(n+\lambda) \\ W_0^{(c)} = \lambda/(n+\lambda) + (1 - \alpha^2 + \beta) \\ W_i^{(m)} = W_i^{(c)} = 1/2(n+\lambda) \quad i = 1, 2, \cdots, 2n \end{cases} \tag{7}$$

where α determines the spread of the sigma points, k is the secondary scaling parameter, and β is used to incorporate prior knowledge of the state distribution[14].

Table 1 Equations of UKF[14]

Parameter	Equation
Initialization	$\boldsymbol{x}^a = [\boldsymbol{x}\ \boldsymbol{w}\ \boldsymbol{\eta}]\ \hat{\boldsymbol{x}}_0^a = E(\boldsymbol{x}^a)$ $\boldsymbol{P}_0^a = \mathrm{diag}[\boldsymbol{P}_0\ \boldsymbol{Q}\ \boldsymbol{R}]\ \boldsymbol{P}_0^a = E(\boldsymbol{x}^a - \boldsymbol{x}_0^a)(\boldsymbol{x}^a - \boldsymbol{x}_0^a)^T$
Sigma point	$\chi^a = \left[\hat{\boldsymbol{x}}_{k-1}^a\ \hat{\boldsymbol{x}}_{k-1}^a + (\sqrt{(n+\lambda)\boldsymbol{P}_{k-1}^a})_i\ \hat{\boldsymbol{x}}_{k-1}^a - (\sqrt{(n+\lambda)\boldsymbol{P}_{k-1}^a})_i\right]$
Sigma point propagation	$\chi_{i,k/(k-1)}^x = \boldsymbol{f}(\chi_{i,k/(k-1)}^x, \chi_{i,k-1}^v), i = 0, 1, \cdots, 2n$
Weighted posterior mean	$\hat{\boldsymbol{x}}_{k/(k-1)} = \sum_{i=0}^{2n} W_i^{(m)} \chi_{i,k/(k-1)}^x$
Weighted posterior covariance	$\boldsymbol{P}_{k/(k-1)} = \sum_{i=0}^{2n} W_i^{(c)} (\chi_{i,k/(k-1)}^x - \hat{\boldsymbol{x}}_{k/(k-1)})(\chi_{i,k/(k-1)}^x - \hat{\boldsymbol{x}}_{k/(k-1)})^T$
Estimated measurement	$\boldsymbol{z}_{i,k/(k-1)} = h(\chi_{i,k/(k-1)}^x, \chi_{i,k/(k-1)}^\eta)$
Weighted measurement mean	$\hat{\boldsymbol{z}}_{k/(k-1)} = \sum_{i=0}^{2n} W_i^{(m)} \boldsymbol{z}_{i,k/(k-1)}$
Weighted measurement covariance	$\boldsymbol{P}_{\hat{z}_k, \hat{z}_k} = \sum_{i=0}^{2n} W_i^{(c)} (\boldsymbol{z}_{i,k/(k-1)} - \hat{\boldsymbol{z}}_{k/(k-1)})(\boldsymbol{z}_{i,k/(k-1)} - \hat{\boldsymbol{z}}_{k/(k-1)})^T$
Cross-correlation covariance	$\boldsymbol{P}_{x_k, z_k} = \sum_{i=0}^{2n} W_i^{(c)} (\chi_{i,k/(k-1)}^x - \hat{\boldsymbol{x}}_{k/(k-1)})(\boldsymbol{z}_{i,k/(k-1)} - \hat{\boldsymbol{z}}_{k/(k-1)})^T$
Kalman gain matrix	$\boldsymbol{\kappa} = \boldsymbol{P}_{x_k, z_k} \boldsymbol{P}_{\hat{z}_k, \hat{z}_k}^{-1}$
State estimate update	$\hat{\boldsymbol{x}}_k = \hat{\boldsymbol{x}}_{k/(k-1)} + \boldsymbol{\kappa}(\boldsymbol{z}_k - \hat{\boldsymbol{z}}_{k/(k-1)})$
Covariance update	$\boldsymbol{P}_k = \boldsymbol{P}_{k/(k-1)} - \boldsymbol{\kappa} \boldsymbol{P}_{\hat{z}_k, \hat{z}_k} \boldsymbol{\kappa}^T$

2.2 Fuzzy regulator design

It is obvious that the estimating accuracy of the magnetic bias is important for the geomagnetic orbit determination. The magnetic bias is influenced by the process noise covariance $\boldsymbol{Q}$. Generally, $\boldsymbol{Q}$ is a constant matrix in UKF.

However, regarding $\boldsymbol{Q}$ as a constant is an approximation. The geomagnetic measurement and the corresponding position data, which are provided by SWARM-A from April 19th to 20th, are utilized to analyze the magnetic bias. The geomagnetic measurement produced by SWARM-A is denoted as B_s, and the geomagnetic magnitude produced by solving the IGRF using SWARM-A position data is denoted as B_c. The difference is defined as

$$\nabla B = B_s - B_c \tag{8}$$

Fig.1 shows the derivative of ∇B, which is denoted as $\nabla\dot{B}$. Obviously, the $\nabla\dot{B}$ changes as satellite orbiting. Thus, it is necessary to utilize a changing $\boldsymbol{Q}$ when performing orbit determination process. A fuzzy regulator is proposed here.

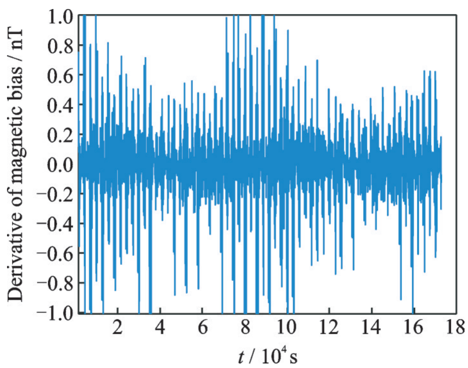

Fig.1 Derivative of magnetic bias

First, when the UKF runs, B_b is estimated. The estimated B_b at t_{k-1} and t_k are denoted as $B_{b,k-1}$ and $B_{b,k}$, respectively. Then, ∇B_b is calculated as

$$\nabla B_b = \left| B_{b,k} - B_{b,k-1} \right| \tag{9}$$

For the geomagnetic orbit determination system, the time update for B_b is

$$B_{b,k+1} = \sum_{i=0}^{2n} W_i^c \left(B_{b,k}^{(c)} + a_{b,k}^{(c)} \right) \tag{10}$$

where $B_{b,k}^{(c)}$ is the sigma points for B_b at t_k and $a_{b,k}^{(c)}$ the sigma points for a_b at t_k.

Since the process covariance matrix $\boldsymbol{Q} = \boldsymbol{w}\boldsymbol{w}^{\mathrm{T}}$, where the process noise $\boldsymbol{w} = [f_x, f_y, f_z, a_b]$. $\boldsymbol{Q}(4, 4)$ is chosen as the output of the fuzzy regulator, which is the element located in the fourth row and the fourth column of the covariance $\boldsymbol{Q}$. Input ∇B_b into the fuzzy regulator, and an adaptive $\boldsymbol{Q}(4, 4)$ is determined. This procedure is called the fuzzy regulator.

The linguistic variables of both ∇B_b and $\boldsymbol{Q}(4, 4)$ are small (S), medium (M), large (L), very large (VL). The membership functions of them are trapezoid. The regulating strategy is shown as follows. When ∇B_b is large, which means B_b changes rapidly and $\boldsymbol{Q}(4, 4)$ should be large. When ∇B_b is close to 0, which means B_b almost remain steady and $\boldsymbol{Q}(4, 4)$ should be small. The corresponding regulating strategy is listed in Table 2.

Table 2 Corresponding control strategy

∇B_b	$\boldsymbol{Q}(4,4)$
S	S
M	M
L	L
VL	VL

A UKF using the afore-mentioned fuzzy regulator is FRUKF in this paper. Its flow chart is shown in Fig. 2. This strategy will improve the estimation accuracy of B_b, and further improve the performance of the geomagnetic orbit determination.

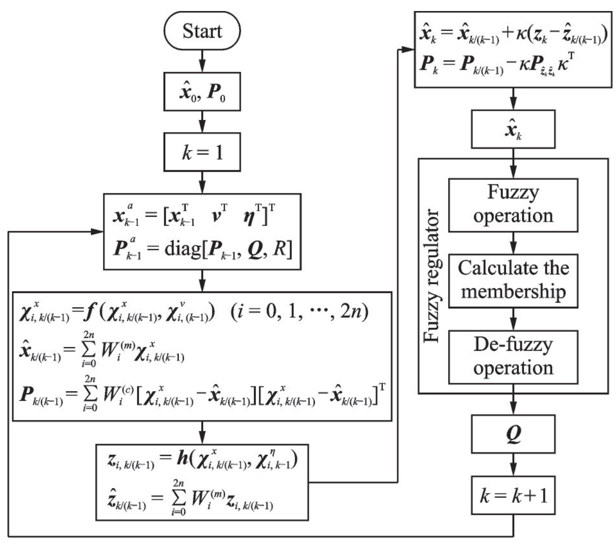

Fig.2 Flow chat of FRUKF

3 Experiments and Analyses

The Swarm mission was launched by the European Space Agency (ESA) on 22 November 2013. The mission consists of three identical satellites, flying in polar orbits. The data for the geomagnetic orbit determination experiments are from SWARM-A, whose initial altitude is about 480 km and inclination is 87.4°. The position accuracy of SWARM-A is better than 0.01 m[15]. Thus, the data from SWARM-A is utilized to evaluate the estimation accuracy of FRUKF.

The orbit determination performance of EKF is first compared with that of UKF. The time span of the experiment data is from April 19th to 20th. $\boldsymbol{x}_0=[\boldsymbol{r}_0, \boldsymbol{v}_0, 0]$, where $\boldsymbol{r}_0$ is the position of SWARM-A with an initial error of 1 000 m, and $\boldsymbol{v}_0=(\boldsymbol{r}_1-\boldsymbol{r}_0)/2$, $\boldsymbol{P}_0$ is set to has a lower order compared to the initial of $\boldsymbol{x}_0$ based on experience. The J2-effect is about 8×10^{-3} m/s², so $\boldsymbol{w}$ is set to be $\boldsymbol{w}=[10^{-4}\ \mathrm{m/s^2}, 10^{-4}\ \mathrm{m/s^2}, 10^{-4}\ \mathrm{m/s^2}, 5\ \mathrm{nT}]$. Therefore, the initial condition of the filter is

$$\boldsymbol{P}_0=\begin{bmatrix} 300^2\boldsymbol{I}_{3\times3} & \boldsymbol{O}_{3\times3} & 0 \\ \boldsymbol{O}_{3\times3} & 0.02^2\boldsymbol{I}_{3\times3} & 0 \\ 0 & 0 & 50^2 \end{bmatrix}$$

$$\boldsymbol{Q}=\begin{bmatrix} 10^{-8}\boldsymbol{I}_{3\times3} & \boldsymbol{O}_{3\times1} \\ \boldsymbol{O}_{1\times3} & 5 \end{bmatrix}$$

$$R=25$$

Set the constants of UKF as $\alpha=1$, $k=0.5$ and $\beta=1.5$, respectively. Fig.3 shows the position errors of both EKF and UKF. The position error is defined as $\left|\boldsymbol{P}_{\mathrm{s}}-\boldsymbol{P}_{\mathrm{f}}\right|$. $\boldsymbol{P}_{\mathrm{s}}$ is the position vector provided by SWARM-A, and $\boldsymbol{P}_{\mathrm{f}}$ the estimated position vector from the filters. Both fEKF and UKF converge at about 60 000 s. After convergence, the position errors of both UKF and EKF vary as orbiting. The max position error of UKF is 7 km, and the max position error of EKF is 10 km. The root-mean-square (RMS) position error of UKF is 3.6 km, and the RMS position error of EKF is 4.6 km. In this paper, all the RMS errors are calculated by using the data after 60 000 s. Therefore, the orbit determination performance of UKF is better than that of EKF. Fig.4 displays the magnetic bias estimation of both EKF and UKF, where the standard deviation (STD) is ∇B defined by Eq.(12). Fig.4 shows that the estimation of the magnetic bias of UKF are similar to that of EKF. The estimation error of magnetic bias is the difference between ∇B and the estimated magnetic bias from filter. The RMS estimation error of magnetic bias is about 22 nT both of EKF and UKF. Since the magnitude of the geomagnetic field varies slowly as orbiting, a small magnetic bias error will introduce a large position error. Therefore, it is meaningful to improve the estimation of magnetic bias.

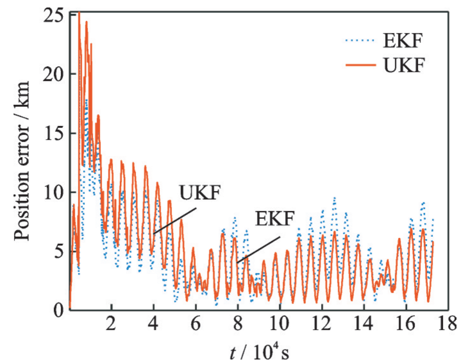

Fig.3 Position errors of EKF and UKF

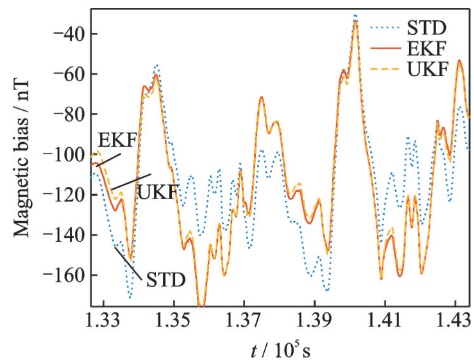

Fig.4 Magnetic biases of EKF and UKF

Fig.5 displays the position errors of UKFs when $\boldsymbol{Q}(4,4)$ changes. All the UKFs converge when time passing, but the time the filters take is different. When $\boldsymbol{Q}(4,4)\leqslant1$, the UKF takes about 20 000 s to converge, but the max position error changes from 10 km to 12 km. When $\boldsymbol{Q}(4,4)$ increase, the filter needs more time to converge, and the position accuracy is improved. When $\boldsymbol{Q}(4,4)>1$, the convergence time the filter takes is about 60 000 s, and the max position error is about 7 km. The detailed results are summarized in Table 3. When $\boldsymbol{Q}(4,4)>5$, the convergence time remains when the position accuracy decreases. Therefore, it is hard to meet the requirement of fast convergence rate and high position accuracy in geomagnetic orbit determination using UKF with a constant covariance $\boldsymbol{Q}(4,4)$. The proposed FRUKF can improve the geomagnetic orbit determination.

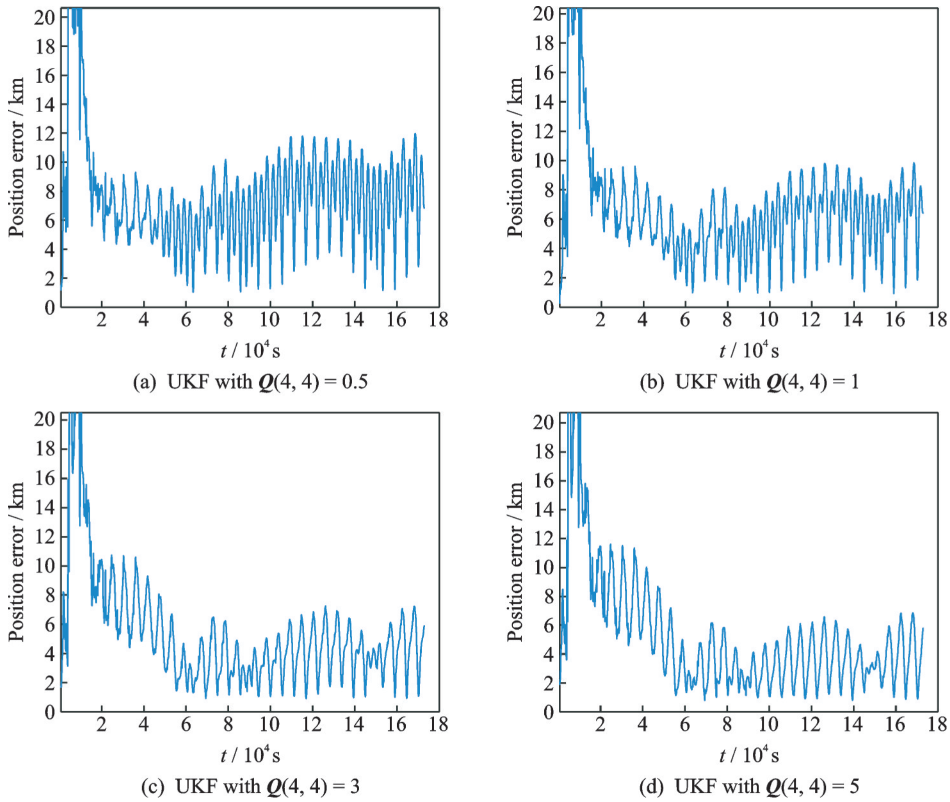

(a) UKF with $\boldsymbol{Q}(4, 4) = 0.5$ (b) UKF with $\boldsymbol{Q}(4, 4) = 1$

(c) UKF with $\boldsymbol{Q}(4, 4) = 3$ (d) UKF with $\boldsymbol{Q}(4, 4) = 5$

Fig.5 Position errors of UKF with different $\boldsymbol{Q}(4,4)$

Table 3 The maximum position error and convergence time using different $\boldsymbol{Q}$

No.	$\boldsymbol{Q}(4,4)$	Max position error / km	Convergence time / s
1	0.3	12	20 000
2	0.5	12	20 000
3	1	10	20 000
4	3	7	60 000
5	5	7	60 000
6	10	7	60 000
7	15	7.5	60 000
8	20	8	60 000
9	50	12	60 000

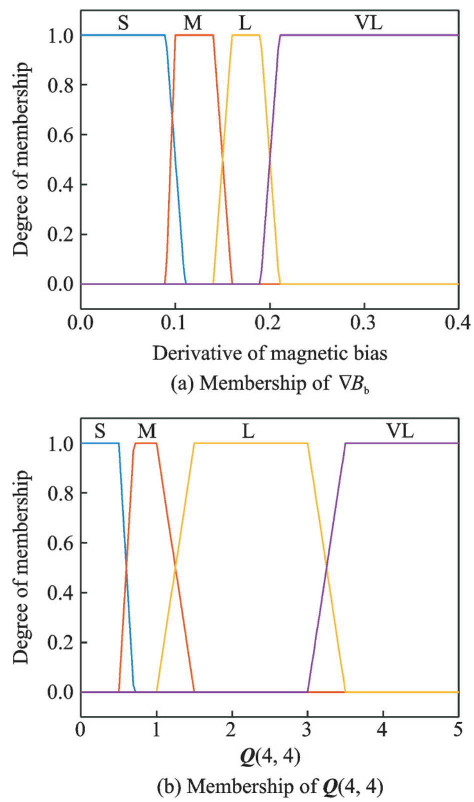

(a) Membership of ∇B_b

(b) Membership of $\boldsymbol{Q}(4, 4)$

Fig.6 Memberships of the fuzzy regulator

The initial conditions of the FRUFK are set to be same to the UKF. Fig.6 is the membership of ∇B_b and $\boldsymbol{Q}(4,4)$. The domain of ∇B_b is $[0,4]$ according to Fig.1 (only partial images are given here), and the domain of $\boldsymbol{Q}(4,4)$ is $\{0.5, 1, 3, 5\}$ according to Table 3. Fig.7 is the position errors of FRUKF and UKF when $\boldsymbol{Q}(4,4)=5$. The system takes 20 000 s to converge, which is as soon as the UKF with $\boldsymbol{Q}(4,4)=0.5$. The maximum position error of UKF when $\boldsymbol{Q}(4,4)=5$ is 7 km, and its RMS position error is 3.6 km. The maximum position error of FRUKF is 6 km, and its RMS position error is 3.1 km. Therefore, the geomagnetic orbit

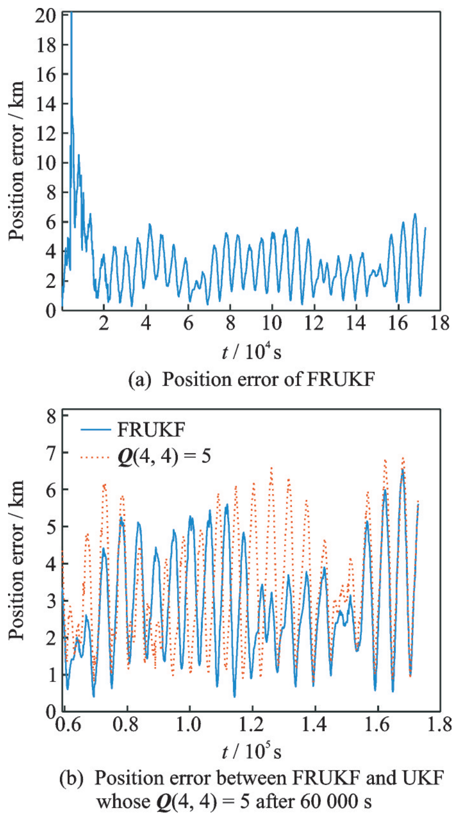

Fig.7 Position error of FRUKF

determination performance of FRUKF is better than the traditional method.

As is shown in Fig.8, the value of $\boldsymbol{Q}(4,4)$ and the slope of bias during the orbit determination have the same trend of change. Therefore, the fuzzy regulator successfully changes the value of $\boldsymbol{Q}(4,4)$ based on the slope of bias. Fig.9 demonstrates the estimation error of geomagnetic bias between FRUKF and UKF. After 60 000 s, the RMS estimation errors of geomagnetic bias of FRUKF and UKF are 16.37 nT and 24.6 nT, respectively. Accordingly, the estimation accuracy of geomagnetic bias of FRUKF is 30% higher than that of UKF.

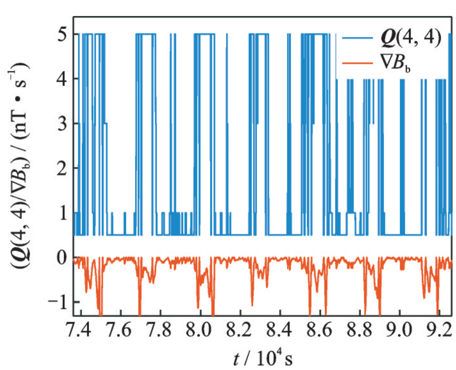

Fig.8 Values of $\boldsymbol{Q}(4,4)$ and $-\nabla B_{\mathrm{b}}$ while orbiting

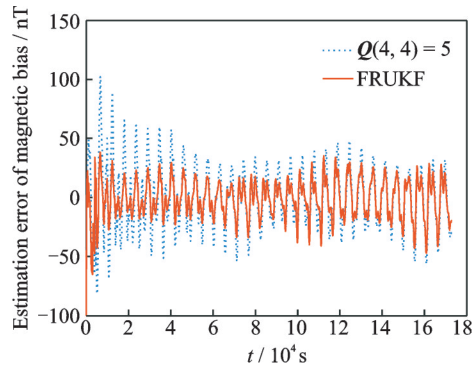

Fig.9 Magnetic errors between FRUKF and UKF when $\boldsymbol{Q}(4,4)=5$

Finally, the calculated amount is compared between UKF and FRUKF. The filters are run in a computer with MATLAB 2019a, and the result is shown in Table 4, where $\boldsymbol{f}(\boldsymbol{x})$ and $\boldsymbol{h}(\boldsymbol{x})$ are the time the state vector and the measurement update take, and the filter time is the time the rest calcultaion of the filter takes. Since the time of data reading and ploting is ignored, the sum of the time of $\boldsymbol{f}(\boldsymbol{x})$, $\boldsymbol{h}(\boldsymbol{x})$ and filter time is shorter than the total time. From Table 4, the time FRUKF takes only increased 19 s, which is 3.2% compared with UKF. Thus, the computational result of FRUKF is similar to that of UKF.

Table 4 Time of running UKF and FRUKF s

Parameter	UKF	FRUKF
$\boldsymbol{f}(\boldsymbol{x})$	130.450	129.854
$\boldsymbol{h}(\boldsymbol{x})$	342.613	344.055
Filter time	75.012	85.129
Totle time	590.825	609.966

4 Conclusions

An FRUKF is proposed for geomagnetic orbit determination. The magnetic bias is modeled as a random walk. The process covariance of the filter is determined on line by a fuzzy regulator according to the trend of magnetic bias estimation. Therefore, the estimation accuracy of the magnetic bias is improved, and then the position accuracy and convergence rate of the filter are also improved. The calculated result of FRUKF is similar to that of UKF. For nanosatellites, it is a useful orbit determination approach.

References

[1] KE Han, WANG Hao, ZHENG Zhonghe. Magnetometer-only linear attitude estimation for bias momentum pico-satellite[J]. Journal of Zhejiang University-Science A: Applied Physics & Engineering, 2010, 11(6): 455-464.

[2] PSIAKI M L, HUANG Lejin, FOX S M. Ground tests of magnetometer-based autonomous navigation (MAGNAV) for low-earth-orbiting spacecraft[J]. Journal of Guidance, Control, and Dynamics, 1993, 16(1): 206-214.

[3] KE Han, WANG Hao, TU Binjie, et al. Pico-satellite autonomous navigation with magnetometer and sun sensor data[J]. Chinese Journal of Aeronautics, 2011, 24(1): 46-54.

[4] ROH K M, PARK E S, CHOI B K, et al. A sigma-point batch filter for spacecraft orbit estimation using the geomagnetic field measurements[J]. Transactions of the Japan Society for Aeronautical and Space Sciences, 2014, 57(4): 201-209.

[5] FARAHANIFAR M, ASSADIAN N. Integrated magnetometer-horizon sensor low-earth orbit determination using UKF[J]. Acta Astronautica, 2015(106): 13-23.

[6] HUA Bing, ZHANG Zhingwen, WANG Feng, et al. FAUKF autonomous orbit determination based on geometric/spectral redshift/sunlight information[J]. Journal of Systems Engineering and Electronics, 2019, 41(1): 154-161.

[7] JUNG H, PSIAKI M L. Tests of magnetometer/sun-sensor orbit determination using flight data[J]. Journal of Guidance, Control, and Dynamics, 2002, 25(3): 582-590.

[8] CHEON Y. Fast convergence of orbit determination using geomagnetic field measurement in target pointing satellite[J]. Aerospace Science and Technology, 2013, 30(1): 315-322.

[9] PSIAKI M L. Autonomous orbit and magnetic field determination magnetometer and star sensor data[J]. Journal of Guidance, Control, and Dynamics, 1995, 18(3): 584-592.

[10] INAMORI T, SHIMIZU K, MIKAWA Y, et al. Attitude stabilization for the nano remote sensing satellite PRISM[J]. Journal of Aerospace Engineering, 2013, 26(3): 594-602.

[11] GHANBARPOURASL H, POURTAKDOUST S H, SAMANI M. A new non-linear algorithm for complete pre-flight calibration of magnetometers in the geomagnetic field domain[J]. Proceedings of the Institution of Mechanical Engineers, Part G: Journal of Aerospace Engineering, 2009, 223(6): 729-739.

[12] GAO Dong, ZHANG Tao, CUI Feng, et al. Development of geomagnetic navigation and study of high precision geomagnetic navigation for LEO satellites [C]//Proceedings of the 2nd China Aerospace Safety Conference, Special Committee on Space And Space Safety Parallel System of Chinese Institute Of Command and Contro. Dalian, China: [s. n.], 2017: 438-445.

[13] THEBAULT E, FINLAY C C, BEGGAN C D, et al. International geomagnetic reference field: The 12th generation[J]. Earth, Planets and Space, 2015, 67(1): 79.

[14] HAYKIN S. Kalman filtering and neural networks [M]. New York: Wiley, 2001.

[15] IJSSEL J, ENCARNACAO J, DOORNBOS E, et al. Precise science orbits for the Swarm satellite constellation[J]. Advances in Space Research, 2015, 56(6): 1042-1055.

Acknowledgement This study was supported by the National Natural Science Foundation of China (No. 61673212).

Authors Mr. **CHEN Guifang** is studying for the master's degree in the College of Astronautics, Nanjing University of Aeronautics and Astronautics. His research interest focuses on autonomous navigation.

Prof. **YU Feng** received the Ph.D. degree in navigation guidance and control from Nanjing University of Aeronautics and Astronautics in 2008. He is currently a professor and doctoral supervisor of the College of Astronautics in Nanjing University of Aeronautics and Astronautics. His main research interest is microsatellite control technology.

Author contributions Mr. **CHEN Guifang** designed the study, complied the models, conducted the analysis, interpreted the result and wrote the manuscript. Prof. **YU Feng** and Prof. **ZONG Hua** contributed to data and the model components for the IGRF model. Ms. **WANG Run** contributed to the discussion and background of the study. All authors commented on the manuscript draft and approved the submission.

Competing interests The authors declare no competing interests.

(Production Editor: ZHANG Tong)

基于模糊调节无迹卡尔曼滤波器的地磁定轨研究

陈贵芳[1,2], 郁 丰[1,2], 踪 华[3], 王 润[1,2]

(1.南京航空航天大学航天学院,南京 211106,中国;
2.空间光电探测与感知工信部重点实验室(南京航空航天大学),南京 210016,中国;
3.宇航智能控制技术国家级重点实验室,北京 100854,中国)

摘要:地磁定轨系统适合于对仪器复用率要求高的微纳卫星使用。考虑到地磁定轨系统的性能受限于地磁偏差,本文设计了模糊调节器,并构建了模糊调节无迹卡尔曼滤波器。将地磁偏差建模为随机游走,并将其变化率作为调节器的输入量,经模糊处理后,自适应调节滤波器的参数。SWARM-A卫星的实测数据实验表明,该算法可有效提升地磁偏差的估计精度,从而提升地磁定轨系统的性能。相较于传统的无迹卡尔曼滤波器,该算法的收敛速度更快,精度也更高,其位置误差均方根值为3.1km.

关键词:地磁定轨;无迹卡尔曼滤波;模糊调节;地磁偏差;国际地磁参考场